

# The DNA Translocating ATPase of Bacteriophage T4 Packaging Motor

Kiran R. Kondabagil, Zhihong Zhang and Venigalla B. Rao\*

Department of Biology, The  
Catholic University of America  
Washington, DC 20064, USA

In double-stranded DNA bacteriophages the viral DNA is translocated into an empty prohead shell by a powerful ATP-driven motor assembled at the unique portal vertex. Terminases consisting of two to three packaging-related ATPase sites are central to the packaging mechanism. But the nature of the key translocating ATPase, stoichiometry of packaging motor, and basic mechanism of DNA encapsidation are poorly understood. A defined phage T4 packaging system consisting of only two components, proheads and large terminase protein (gp17; 70 kDa), is constructed. Using the large expanded prohead, this system packages any linear double-stranded DNA, including the 171 kb T4 DNA. The small terminase protein, gp16 (18 kDa), is not only not required but also strongly inhibitory. An ATPase activity is stimulated when proheads, gp17, and DNA are actively engaged in the DNA packaging mode. No packaging ATPase was stimulated by the N-terminal gp17-ATPase mutants, K166G (Walker A), D255E (Walker B), E256Q (catalytic carboxylate), D255E-E256D and D255E-E256Q (Walker B and catalytic carboxylate), nor could these sponsor DNA encapsidation. Experiments with the two gp17 domains, N-terminal ATPase domain and C-terminal nuclease domain, suggest that terminase association with the prohead portal and communication between the domains are essential for ATPase stimulation. These data for the first time established an energetic linkage between packaging stimulation of N-terminal ATPase and DNA translocation. A core pathway for the assembly of functional DNA translocating motor is proposed. Since the catalytic motifs of the N-terminal ATPase are highly conserved among >200 large terminase sequences analyzed, these may represent common themes in phage and herpes viral DNA translocation.

© 2006 Elsevier Ltd. All rights reserved.

**Keywords:** phage T4; virus assembly; DNA translocation; terminase; DNA packaging

\*Corresponding author

## Introduction

Genome packaging occupies a central position in the morphogenesis of double-stranded (ds) DNA bacteriophages and herpes viruses. It transitions the virus from a highly metabolically active replicative state to an inactive extracellular state that preserves the integrity of the genetic material. Packaging is initiated through recognition and endonucleolytic cleavage of viral concatemeric DNA by a multi-

subunit complex known as the terminase, which in phage T4 is constituted by the small subunit gp16 (18 kDa) and the large subunit gp17 (70 kDa).<sup>1,2</sup> The terminase links the cleaved DNA to the dodecameric portal (gp20, 61 kDa) situated at the unique vertex of the empty prohead. The packaging machine thus assembled utilizes ATP free energy to drive directional translocation of DNA into the capsid through the portal pore.<sup>3,4</sup> When a limiting, almost crystalline, density of packed DNA is reached, tight spooling of DNA around the portal apparently signals packaging termination,<sup>5</sup> triggering a second nucleolytic cleavage and dissociation of the terminase-DNA complex from the DNA-full head. These packaging events occur processively through gp16-mediated recognition of viral genome and assembly of a supramolecular packaging machine.<sup>6</sup>

Abbreviations used: aa, amino acid(s); ds, double-stranded; ELPs, empty large particles; ESPs, empty small particles; gp, gene product(s).

E-mail address of the corresponding author:  
[rao@cua.edu](mailto:rao@cua.edu)

The basic mechanism of DNA translocation is poorly understood. The model favored by many is the symmetry mismatch model,<sup>7</sup> which postulates that the mismatch between the 5-fold capsid and 12-fold portal allows ATP-driven portal rotation that is coupled to DNA translocation. Based on the cryo-EM imaging and atomic structure of phage Phi-29 portal, a refined symmetry mismatch model was suggested in which the subunits of a pentameric ATPase “fire” sequentially, promoting compression and relaxation of the portal that is coupled to DNA movement.<sup>8</sup> As much as 57 piconewtons force, about 20–25 times greater than that of myosin motor, is generated by the DNA packaging motor, making it one of the strongest biological machines reported to date.<sup>9</sup> The best estimates suggest that the Phi-29 motor translocates an average of 2 bp of DNA per one ATP hydrolysis.<sup>10</sup> If the same is true for phage T4 motor, approximately 10<sup>5</sup> molecules of ATP would be utilized to package one molecule of T4 DNA.

Although a translocating ATPase is central to the DNA packaging mechanism, the ATPase center that powers DNA translocation has not been definitively established. Two to three packaging-related ATPase sites have been identified in many phage terminases including T4.<sup>11,12</sup> Previous mutagenesis studies showed that the N-terminal ATPase site, but not the second putative ATPase site in the central portion of gp17, is critical for function.<sup>13</sup> We have extensively characterized the N-terminal ATPase center, which is highly conserved among numerous phage and viral terminases.<sup>14</sup> Accumulated evidence implicates this ATPase in DNA packaging: (i) gp17 alone exhibits ATPase and *in vitro* DNA packaging activities, which are stimulated 50–100-fold by the small terminase, gp16;<sup>15</sup> (ii) no mutations are tolerated in the proposed catalytic residues of the N-terminal Walker A (SRQLGKT<sub>161–167</sub>),<sup>13</sup> Walker B (MIYID<sub>251–255</sub>),<sup>16</sup> catalytic carboxylate (E256)<sup>17</sup> and ATPase coupling (TTT<sub>285–287</sub>) motifs;<sup>14</sup> (iii) highly conserved substitutions result in a loss of gp16-stimulated ATPase and *in vitro* DNA packaging activities.<sup>13,15–17</sup>

A direct energetic linkage between the N-terminal ATPase center and DNA translocation is however lacking in any system. Since the T4 *in vitro* DNA packaging is measured as the number of infectious viruses produced, the observed DNA packaging defects in gp17 mutants could be due to pre or post-packaging defects, but not necessarily due to defective DNA translocation *per se*.<sup>16</sup> In fact, Dhar and Feiss reported two gpA mutants in gpA N-terminal ATPase, Y46F and K84E, which showed a loss of viral infectivity by six orders of magnitude due to post-packaging assembly defects but their DNA packaging and ATPase activities remained largely intact.<sup>18</sup>

Here, we show that a defined T4 *in vitro* packaging system consisting of only two components, purified proheads and gp17, can efficiently package linear dsDNA. An ATPase activity is strongly stimulated only upon the assembly of a

functional DNA packaging motor. This ATPase stimulation was observed in the absence of gp16, which is known to robustly stimulate gp17-ATPase.<sup>15,19</sup> None of the N-terminal gp17-ATPase mutants could package DNA, or be stimulated by proheads and DNA. Terminase association with the prohead (portal) and communication between the two gp17 domains, the N-terminal ATPase domain and the C-terminal nuclease domain, is critical for packaging ATPase stimulation. These data for the first time establish an energetic linkage between the N-terminal gp17-ATPase and DNA translocation and provide insights on the mechanism of packaging initiation and assembly of a functional packaging motor.

## Results

### DNA packaging components

In order to construct a defined packaging system, highly purified packaging components, wild-type and mutant gp17s (Figure 1), gp16, and proheads were prepared by a combination of Ni-affinity, ion-exchange, and size-exclusion chromatographies. The gp17-K577 protein (amino acid (aa) residues 1–577), truncated by deleting the C-terminal 33 aa, was used as the wild-type as it retained essentially all the biological functions of the full-length protein.<sup>17</sup> But, unlike the full-length protein, which is non-specifically cleaved at the C terminus during purification to generate two–three truncated species (Figure 2(a), lanes 6–9),<sup>15</sup> gp17-K577 is protease-resistant and migrated as a single band by SDS-PAGE (Figure 2(a), lane 2) and allowed precise data quantification. The purified N360 (ATPase) and C360 (nuclease) domains,<sup>20</sup> Walker A (K166G), Walker B (D255E), and catalytic carboxylate (E256Q) mutants, the double mutants D255E-E256D<sup>15–17</sup> and D255E-E256Q (newly constructed for this study) (Figure 2(a), lanes 3–10), which are deficient in one or more of gp17 functions (Figure 1, right panel), were used to dissect the defined packaging system.

Based on our previous study, which showed that the T4 expanded proheads (ELPs), but not unexpanded proheads (ESPs), efficiently packaged DNA *in vitro*, a preparation enriched for ELPs was isolated from cells infected with *17am18am* mutant at 37 °C<sup>21</sup> (Figure 2(c), lanes 3 and 4). The *18am* mutation (gp18: major tail sheath protein, 71 kDa) was included to prevent premature tailing of empty proheads, which was observed at high frequency in the *17am* (*18*<sup>+</sup>) infected cells.<sup>22</sup> Mono-Q column separated the proheads into two peaks, a sharp peak consisting of pure ELPs (Figure 2(b), Peak 1) followed by a broad peak (Figure 2(b), Peak 2) consisting of mostly ELPs and a small fraction of ESPs (many of the ESPs apparently expanded during purification resulting in a broad peak). The proheads showed one major band corresponding to

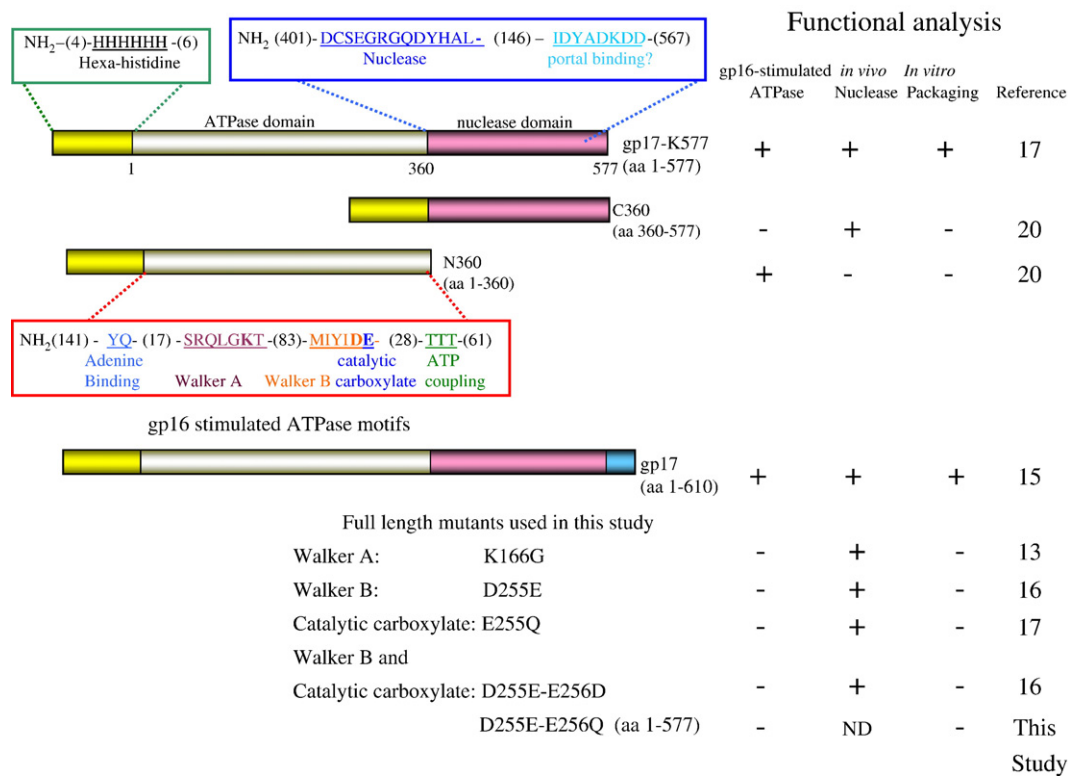


**Figure 1.** Schematic of gp17 constructs and their functional properties. The basic features of each segment of the recombinants are shown in the rectangular boxes; numbers in parentheses represent the number of aa; the N-terminal ATPase motifs, Walker-A, Walker-B, and catalytic carboxylate, are shown. Further details were as described.<sup>14–17,20</sup> The functional properties of the constructs are indicated on the right; +, retain activity; –, no activity detected; ND, not determined.

the major capsid protein, gp23\*, but no gp18 (Figure 2(c), compare lane 5 with lane 2) attesting to the high purity; no non-specific ATPase activity was detectable with the purified proheads (see below). The Peak-1 ELPs exhibited 15–20% greater DNA packaging activity than Peak-2 (ELPs+ESPs) and were used for all the experiments performed in this study. Yields of ELPs were about  $4 \times 10^{12}$ – $5 \times 10^{12}$  particles per liter of infected cells.

### The two-component DNA packaging system

Although phage T4 is the largest of the well-characterized dsDNA phages, the defined *in vitro* packaging system turned out to be quite a simple one, in fact the simplest of the reported systems.<sup>23–25</sup> The complete system consisted of only two essential components, ELPs and gp17-K577 (Figure 3(a)). These (ELPs, 0.3 nM ( $2 \times 10^9$  proheads); gp17-K577, 1  $\mu$ M) were mixed with the 29 kb BamH1-linearized pAD10 plasmid DNA<sup>26</sup> (1 nM;  $1 \times 10^{10}$  molecules) in the presence of ATP (0.75 mM) and standard buffer components<sup>27</sup> (Tris-Cl (pH 7.5),  $Mg^{2+}$ , polyamines, PEG, NaCl) to assemble the functional DNA packaging machine. Typically, under these conditions of excess gp17 and ATP, about 12% of the input pAD10 DNA was packaged, i.e. remained DNase resistant. In numerous control experiments in which either ELPs, gp17, or both were omitted, no DNase protection was observed (Figure 3(a)).

ATP is absolutely required for packaging since no detectable DNA packaging occurred in its absence (Figure 3(b), lane 5). Hydrolysis of ATP, not its mere presence, is necessary for packaging DNA. No packaging was observed in the presence of three different non-hydrolyzable analogs, ATP- $\gamma$ -S, AMP-PNP, and AMP-PCP (Figure 3(c), lanes 2–4). When ATP- $\gamma$ -S was added to the complete reaction (containing ATP), packaging was inhibited with increasing concentration of the analog, reaching 96% inhibition at 2 mM (Figure 3(c) lanes 7–9). Packaging was optimal at pH 7.5 (Figure 3(b), compare lanes 11 and 12 with 2) and enhanced by polyamines (Figure 3(b) lane 6–9). Polyethylene-glycol (PEG), which promotes macromolecular crowding in the reaction mixture, was a potent enhancer of DNA packaging (Figure 3(b) compare lane 10 with lane 2). The small terminase protein, gp16, on its own does not possess any packaging activity (data not shown). However, surprisingly, gp16 which stimulates gp17-ATPase and *in vitro* DNA packaging in the crude system (50–100-fold),<sup>15</sup> showed a dramatic inhibition of DNA packaging in the defined system (Figure 3(b) compare lane 3 with lane 2). When a gp16:gp17 molar ratio of 8:1 (optimal ratio for ATPase stimulation) was used, packaging efficiency was reduced by >80%. Further increase in gp16 completely abolished DNA packaging (data shown; see Figure 5).

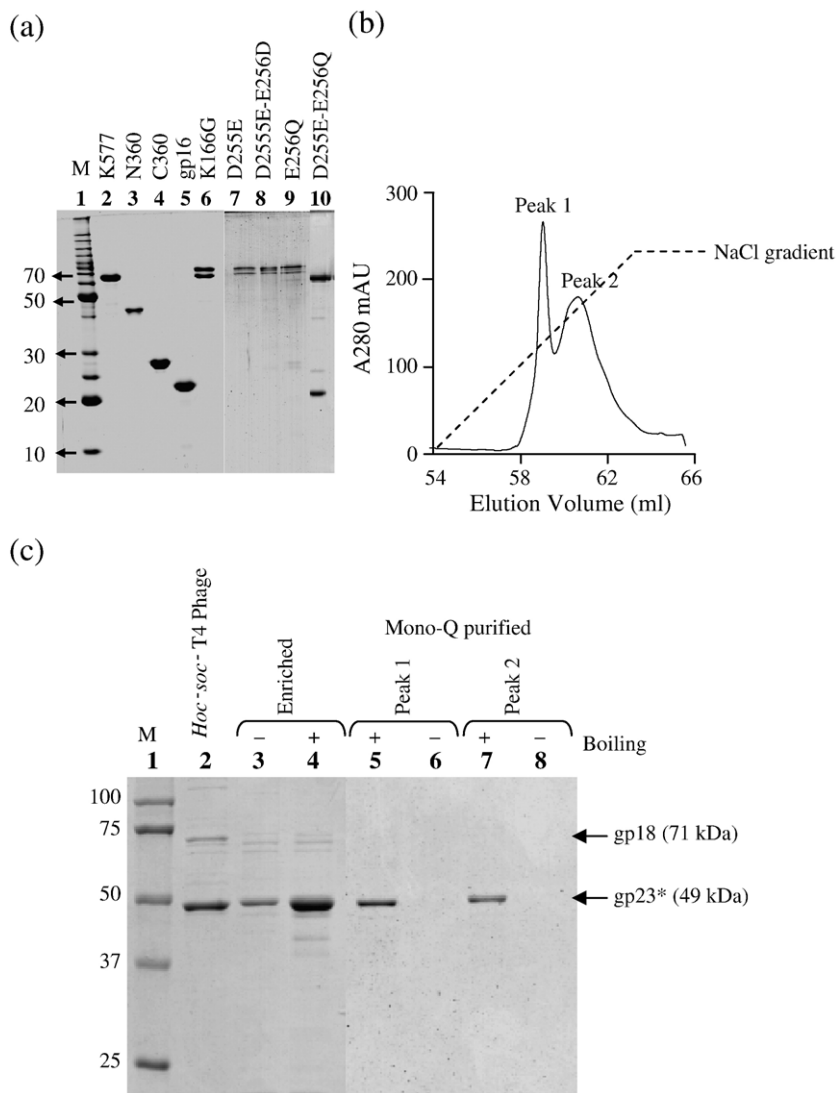


**Figure 2.** Purification of proheads and terminase proteins. (a) SDS-PAGE showing the purity of gp17-K577, gp16, gp17 domains and mutants. Lane M shows the standard protein markers. (b) Mono-Q column elution profile of proheads. Proheads were applied onto a Mono-Q Column (Mono Q 5/50 GL; GE Healthcare) pre-equilibrated with 50 mM Tris (pH 7.5), 3 mM  $\beta$ -mercaptoethanol, 5 mM  $MgCl_2$ . Bound proheads were eluted with 0–400 mM linear NaCl gradient (broken line). (c) Determination of the expanded state of proheads. Mono-Q peak fractions following concentration by high-speed centrifugation were electrophoresed on 12% SDS-PAGE. The samples were treated with SDS-sample buffer for 5 min either at room temperature (unboiled; –) or in a boiling water bath (boiled; +) prior to electrophoresis. Enriched represents the proheads isolated by differential centrifugation, i.e. the fraction that was loaded onto the Mono-Q column. A known amount of *hoc<sup>-</sup>soc<sup>-</sup>* phage (lane 2) was used in each experiment and gp23\* band was quantified to determine the number of prohead particles in a given sample.

### The purified ELPs efficiently package DNA in the defined system

Like the crude *in vitro* DNA packaging system,<sup>28</sup> the defined system exhibited temperature sensitivity; optimal temperature for packaging was at ~30 °C whereas at 38 °C, packaging dropped to 40% (Figure 4(a)). More than 50% of the packaged DNA, i.e. about 7.5% of the input DNA, was packaged within the first 12 min of incubation, reaching completion by about 45 min (Figure 4(b)). Packaging lagged at low gp17 concentration and increased linearly after a threshold concentration (0.5–1  $\mu$ M) was reached (Figure 4(c)). This sigmoidal behavior is consistent with the hypothesis that gp17 cooperatively assembles into a higher order packaging motor complex on the prohead portal.<sup>27</sup> Kinetics of this assembly and stoichiometry of the packaging complex, which remained unresolved in any packaging system, are being investigated (see Figure 7). Optimal ATP concentration was about 0.75 mM, and similar to what was observed with the gp16-stimulated gp17-ATPase,<sup>15</sup> slight inhibition

was observed at concentrations above 2 mM ATP (Figure 4(d)).

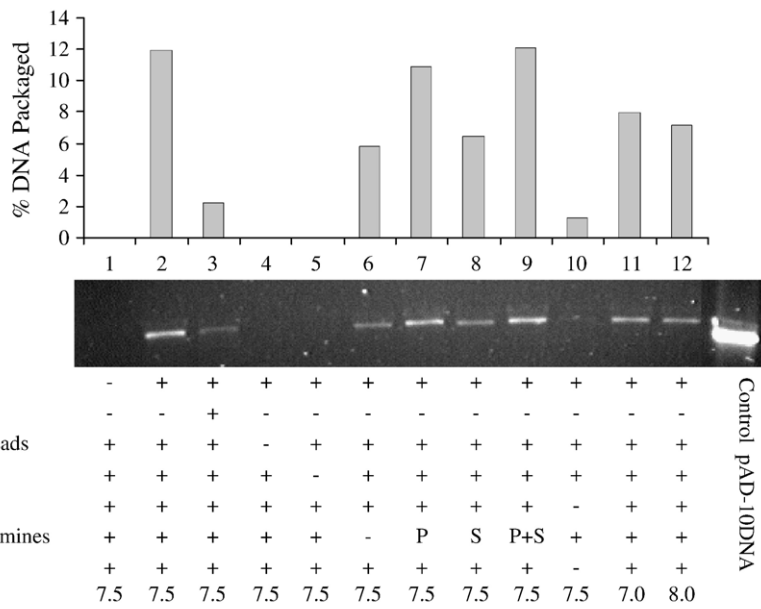
The purified ELPs exhibited high packaging efficiency† in the defined system, relative to the crude *in vitro* systems described earlier (Figure 4(e)).<sup>21,27</sup> Prohead filling increased with increasing prohead concentration. Up to ~30% of ELPs or DNA could be packaged under optimal conditions (e.g. 0.075 nM proheads ( $0.5 \times 10^9$  particles), 1.5  $\mu$ M gp17 and 1 nM pAD10 DNA ( $1 \times 10^{10}$  molecules); see Figure 4(e) and data not shown), whereas in the crude system where the packaging efficiency was measured as plaque forming units, the efficiency

† The prohead packaging efficiency is defined as the percentage of input proheads packaged, assuming that one molecule of pAD10 DNA is packaged per prohead. Thus, the number of DNA molecules packaged (as determined from agarose gel quantification) is equivalent to the number of proheads packaged; the total number of proheads was determined by quantification of the gp23\* band following SDS-PAGE; see Materials and Methods.

(a)

<i>In vitro</i> DNA packaging components	Packaging efficiency (%)
Complete	100
- gp17	0
- Proheads	0
- ATP	0
+ATP- $\gamma$ -S	4.1
- polyamines	8
- PEG	27.6
+ gp16	18.9

(b)



(c)

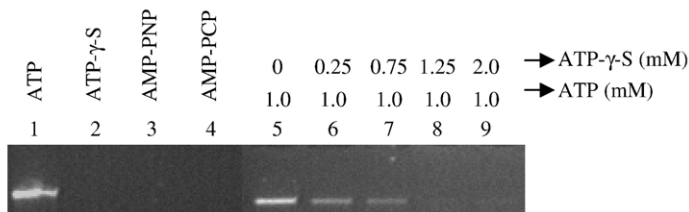


**Figure 3.** Components of the phage T4 defined *in vitro* DNA packaging system. (a) Basic requirements for DNA packaging. The amount of DNA packaged in each case was determined by comparing it with the complete reaction mixture (100%) wherein ~12% of the added pAD10 DNA was packaged. (b) Agarose gel showing the DNase-resistant pAD10 DNA recovered following packaging. Top panel shows a bar diagram of the percent DNA packaged. The presence (+) or absence (-) of individual components in the packaging reaction mixture is indicated below the respective lane. Each packaging reaction contained a positive control (complete reaction mixture), a negative control (minus proheads), and DNA marker (last lane) to quantify the percent DNA packaged in the respective experiment. P, putrescine (1 mM) only; S, spermidine (1 mM) only; P+S, both putrescine and spermidine (1 mM each). (c) DNA packaging in the presence of ATP analogs. 1 mM ATP or analog was used in a standard packaging reaction mixture (lanes 1–4). Packaging inhibition experiment (lanes 5–9) was carried out by varying the ATP- $\gamma$ -S concentration from 0.25 to 2.0 mM while keeping the ATP concentration constant at 1 mM.

was 0.01–1%.<sup>21</sup> It should however be noted that some of the proheads are likely filled with more than one pAd10 DNA molecule (29 kb; less-than headful length) as was previously reported in the crude *in vitro* DNA packaging system (see Discussion).<sup>29</sup> Finally, it is quite remarkable that the proheads retained full packaging-competency after repeated freezing and thawing as well as storage for 12 years at  $-70^{\circ}\text{C}$  (data not shown). Presumably, capsid expansion and addition of two outer capsid proteins, Soc and Hoc,<sup>30</sup> rendered the T4 proheads

an extremely stable packaging-competent protein container.

### DNA specificity

The defined packaging system showed no specificity for a particular DNA sequence. All four unrelated linear dsDNAs, pAD10 (BamH1-linearized; 29 kb), phage  $\lambda$  (48 kb), phage T4 (171 kb) and pET28b (BamH1-linearized; 5.4 kb) were packaged by the defined system (Figure 5(a)). As mentioned

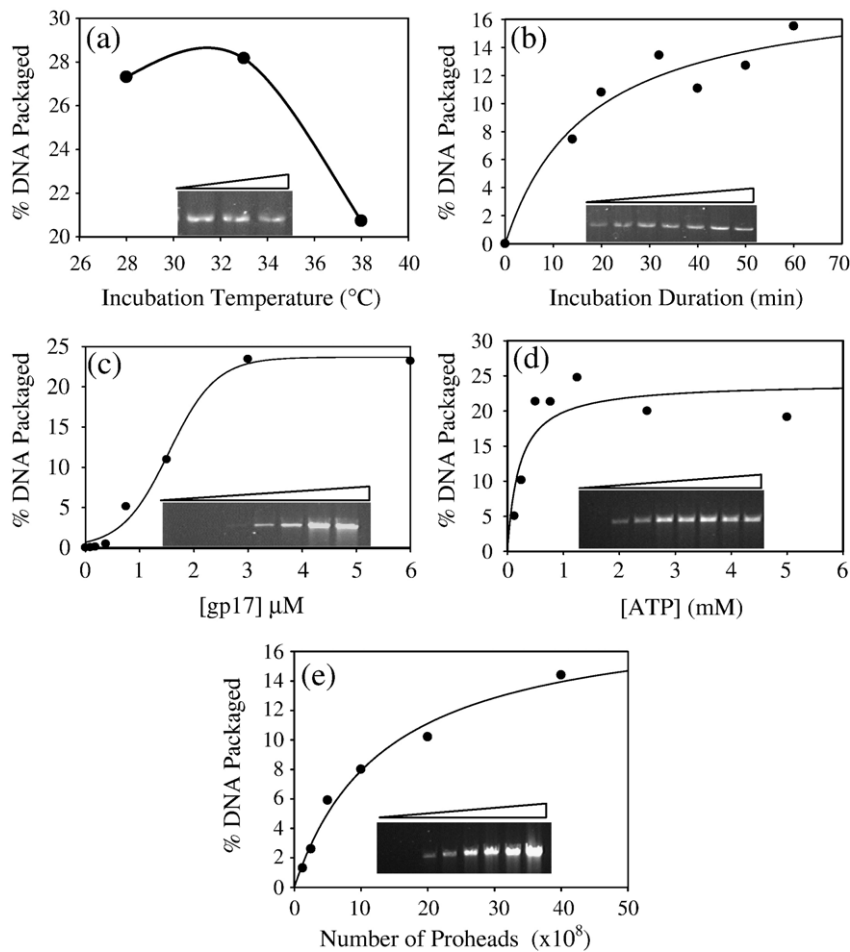


**Figure 4.** Parameters for defined DNA packaging. Packaging assays were carried out as described in Materials and Methods by varying one component or condition in each experiment. Percentage of DNA packaged is plotted as a function of (a) incubation temperature, (b) incubation duration, (c) gp17-K577 concentration, (d) ATP concentration, and (e) prohead concentration. Agarose gel corresponding to each variable is shown as an inset in each panel.

above, packaging was greatly diminished in each case in the presence of gp16 (Figure 5(a); compare lanes 4, 7, 10, 13 with lanes 3, 6, 9, 12, respectively). The size of the packaged DNA corresponded to the linear substrate used, suggesting packaging initiation at the ends of the linear DNA. No significant shorter fragments were observed, which means that internal initiation was not highly significant. Interestingly, several uncut circular plasmid DNA molecules were also packaged, however the efficiency was generally lower than that of the linear DNA. These include the 2.7 kb pUC19, 3.3 kb pUC19-GFP, 5.4 kb pET28b, and 29 kb pAD10 (Figure 5(b)). In each case, the size of the packaged DNA corresponded to the respective linear monomeric form (Figure 5(b) and (c))<sup>‡</sup>. To test whether packaging was primed by nicks that may be present in the circular plasmid, the pUC19, pET28b, and pAD10, plasmid DNAs were ligated to seal off the nicks prior to DNA packaging. In independent experiments, the ligated circular DNA was packaged as well as the unligated DNA (Figure 5(b) lane 6 and data not shown). Gp16 also inhibited the encapsidation of circular DNAs (Figure 5(b) lanes 4, 7, 11, 14 and 17).

<sup>‡</sup> The faint high molecular mass band present in lanes 10, 13, and 16, presumably represents the packaged multimeric plasmid DNA and/or *E. coli* chromosomal DNA fragments present in the plasmid DNA preparation.

It is likely that the circular plasmids were first cut and then packaged from the newly generated end. This hypothesis is consistent with the fact that the T4 gp17 possesses nuclease activity that non-specifically cuts plasmid DNAs *in vivo*. To analyze this further, the packaged circular pAD10 DNA was cut with ScaI. Since the original cut on the circular plasmid was expected to occur randomly and ScaI has a unique cleavage site in pAD10, ScaI cutting should generate a smear of DNA fragments. This indeed was the case (Figure 5(c) lane 4). The same was also observed when packaged circular pET28b DNA was cut with PshAI (Figure 5(c) lane 8). On the other hand, ScaI and PshAI cleavage of the packaged linear pAD10 and pET28b DNAs generated sharp DNA fragments (Figure 5(c) lanes 5 and 9; the second 4 kb ScaI fragment was faint and did not reproduce well in lane 5), the length of which precisely corresponded to what was expected if packaging was initiated at the BamHI end.

### Stimulation of a packaging ATPase

A central hypothesis in the packaging models is that a specific ATPase is activated following the assembly of functional packaging motor.<sup>1-4</sup> Thus far this has been difficult to establish in any phage system because: (i) there are two–three ATPase sites in terminases,<sup>11,12</sup> (ii) the small terminase stimulates

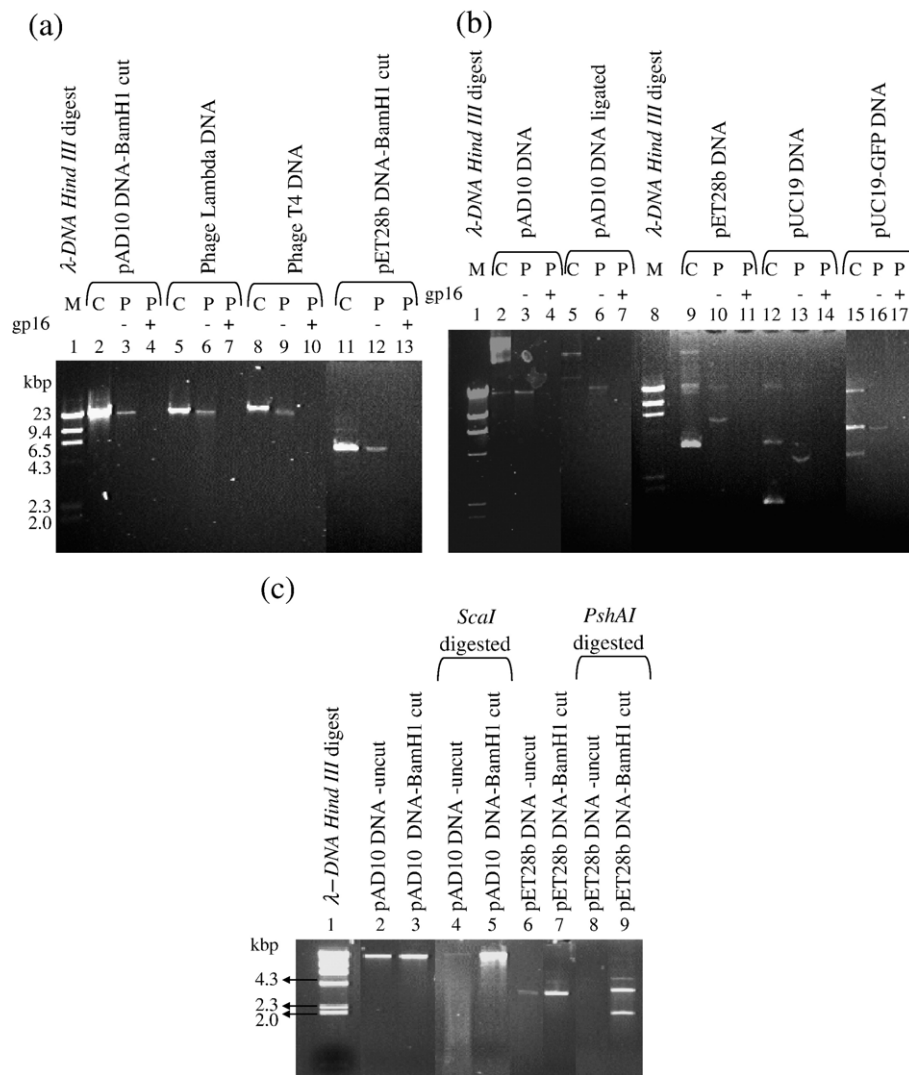


**Figure 5.** DNA packaging specificity. Proheads ( $0.3 \text{ nM}$ ,  $2 \times 10^9$  particles) and gp17 ( $1.5 \text{ }\mu\text{M}$ ) were incubated with various linear (a) or circular (b) DNAs ( $1 \text{ nM}$ ,  $1 \times 10^{10}$  molecules) with (+) or without (-) gp16 ( $12 \text{ }\mu\text{M}$ ) and DNA packaging was performed as described in Materials and Methods. The pAD10 and pET28b DNAs were linearized with BamHI. Ligated DNA was prepared by treating the uncut plasmid DNAs with T4 DNA ligase overnight at  $16 \text{ }^\circ\text{C}$ . Lanes C represent control uncut plasmid DNAs, and lanes P, packaged DNA. (c) The circular (uncut) or linear (BamHI cut) pAD10 (lanes 2–5) and pET28b (lanes 6–9) were first packaged by the standard procedure. For lanes 4, 5, 8 and 9, the respective packaged DNA from several reactions were pooled and the DNA was isolated by ammonium acetate precipitation and treated with *ScaI* in the case of pAD10 and *PshAI* in the case of pET28b for 2 h at  $37 \text{ }^\circ\text{C}$ .

the large terminase-ATPase in the absence of DNA packaging,<sup>15,19,31</sup> and (iii) the small terminase and prohead may possess non-packaging ATPase activity.<sup>18,32</sup> Since the T4 defined packaging system is independent of gp16 (Figure 3), it provided a unique experimental stage to analyze this hypothesis without the complication of packaging-independent ATPase stimulation by the small terminase.

The data clearly showed that an ATPase is activated only when all the packaging components, proheads, large terminase, and DNA, are present in the reaction mixture (Figure 6(a) K577 panel, lanes 7 and 8) and DNA packaging occurred (agarose gel inset, lanes 7 and 8). If any of the components were missing, no DNA packaging occurred and only a weak basal ATPase activity was observed (Figure 6(a) lanes 2–6). Thus there was a strict correlation

between ATPase stimulation and DNA encapsidation. Quantitative data showed that the packaging ATPase stimulation was up to eight to tenfold§.

### The N-terminal ATPase mutants lack packaging ATPase

Five conservative mutants in the catalytic pocket of the N-terminal ATPase center, K166G (Walker A

§ This may not reflect the “true” fold-stimulation of packaging-ATPase under the most optimal conditions, using high concentrations of the packaging components. Since this would generate high non-specific radioactive background, alternative ATPase assay methods are being developed to rigorously quantify the kinetic parameters of DNA translocation.

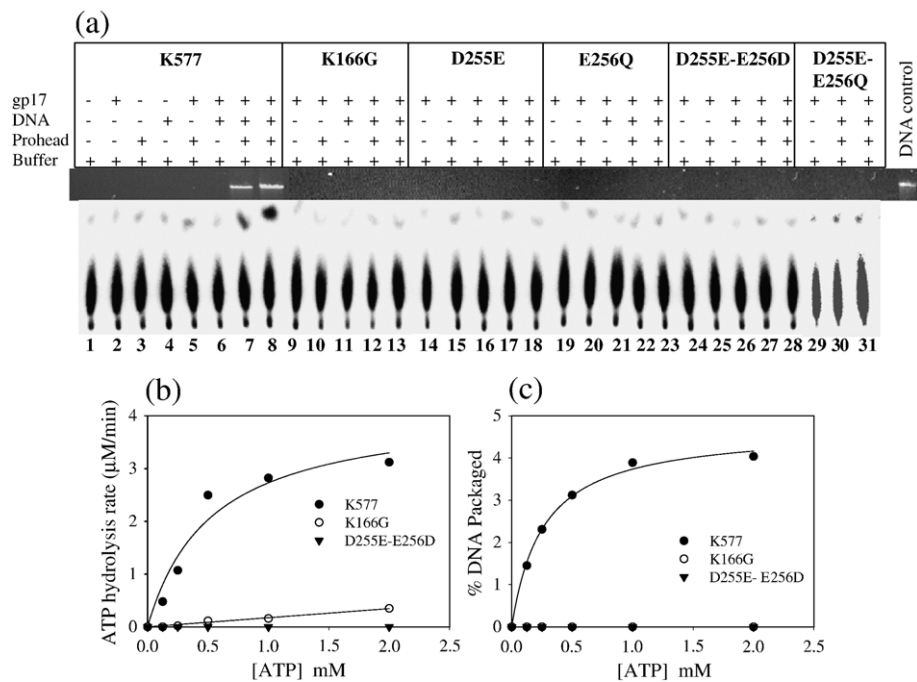


**Figure 6.** DNA packaging stimulates N-terminal gp17-ATPase. (a) Autoradiogram showing the hydrolysis of ATP by wild-type gp17-K577 and ATPase mutants, K166G, D255E, D255E-E256D E256Q and D255E-E256Q. The inset shows the agarose gel depicting the amount of DNA packaged under each condition. The presence and absence of a component is indicated by + and - symbols, respectively. In separate experiments, the ATPase activity (b) and the amount of DNA packaged (c) were quantified at varying concentration of ATP. The ATPase assays were performed as described in Materials and Methods using proheads ( $0.3 \text{ nM}$ ,  $2 \times 10^9$  particles), gp17 or mutants ( $0.5 \text{ }\mu\text{M}$ ), linear pAD10 DNA ( $1 \text{ nM}$ ,  $1 \times 10^{10}$  molecules), and  $1 \text{ mM}$  ATP plus  $75 \text{ nM}$  of [ $\gamma$ - $^{32}$ P]ATP.

mutant); D255E (Walker B mutant); E256Q (catalytic carboxylate mutant); D255E-E256D and D255E-E256Q (Walker B plus catalytic carboxylate mutant); were tested to analyze the linkage between this ATPase and DNA packaging. All the mutants consistently failed to show significant stimulated-ATPase or DNA packaging activities (Figure 6(a), lanes 9–31; the low ATPase activity observed with the K166G mutant in Figure 6(b) was likely due to a minor contaminant, as this mutant has been well established to lack the stimulated ATPase activity).<sup>13</sup> Increasing the ATP concentration up to  $2.0 \text{ mM}$  or gp17 concentration up to 12 times more than wild-type ( $6 \text{ }\mu\text{M}$ ; data not shown) did not lead to ATPase stimulation (Figure 6(b)) or DNA packaging (Figure 6(c)).

### The split domains of large terminase possess no packaging stimulated ATPase

The T4 large terminase can be split into two functional domains: N-domain (aa 1–360) that retains the gp16-stimulated ATPase activity and C-domain (aa 360–577) that retains the nuclease activity.<sup>20</sup> Both domains were analyzed for basal ATPase, gp16-stimulated ATPase, packaging stimulated ATPase, and DNA packaging, as a function of ATP concentration. As reported earlier, the N-domain, but not the C-domain, retained the gp16-stimulated ATPase activity (Figure 7(a), lanes 6 and 9). However, neither domains (even up to  $6 \text{ }\mu\text{M}$ ),

more importantly the ATPase domain, failed to show any packaging-stimulated ATPase and exhibited no DNA packaging activity (Figure 7(a) lanes 5 and 8 and Figure 7(b)). Addition of both the domains together did not restore the activities either (data not shown). On the other hand, addition of domains to the packaging reaction mixture inhibited the gp17-K577-dependent DNA packaging (Figure 7(c)). The C-domain is a much stronger inhibitor than the N-domain.

## Discussion

A two-component bacteriophage T4 defined DNA packaging system, the simplest and one of the most efficient of such systems, is described. Packaging up to about 30% of the added proheads or DNA, this system does not discriminate the DNA substrate based on sequence and can package up to 171 kb T4 DNA, the headful size of prolate bacteriophage T4.

The two packaging components of the defined system are: (i) the truncated gp17-K577 large terminase and (ii) *17am18am* proheads. Unlike phages T3 and  $\lambda$  wherein the C-terminal 30 aa of the large terminase are essential for portal interaction,<sup>33,34</sup> the C-terminal 33 aa of T4 large terminase appears to form a “floppy” extension. They are sensitive to non-specific proteolysis and clearly dispensable for *in vitro* DNA packaging. However, like the T3 and  $\lambda$  phages, the C-terminal domain of

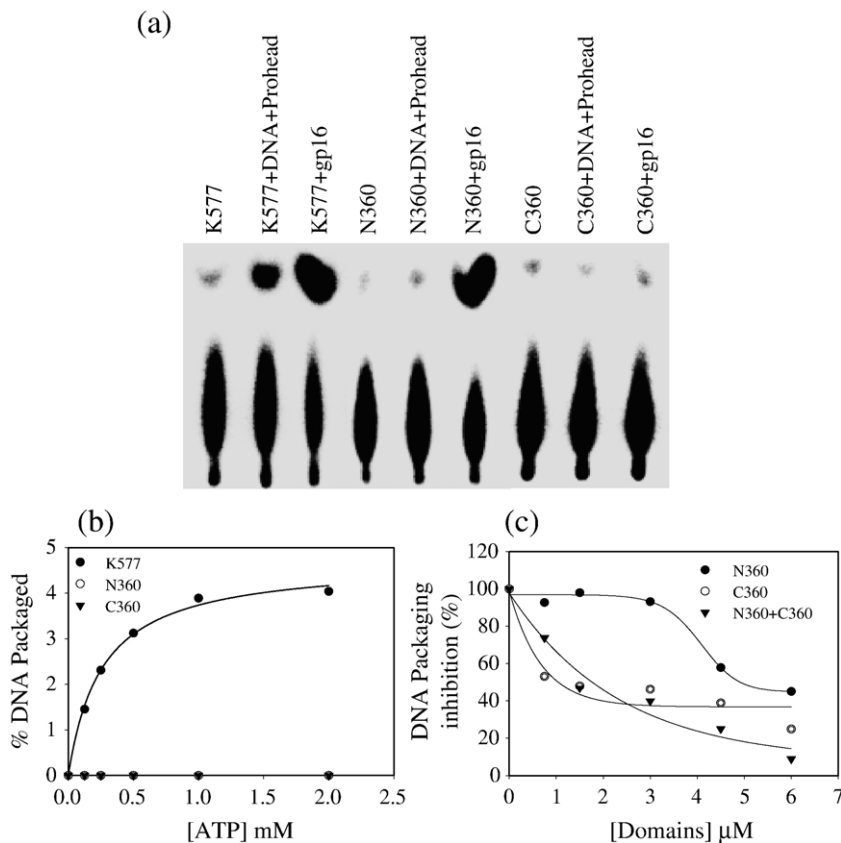


**Figure 7.** Communication between the gp17 domains is essential for packaging ATPase stimulation. (a) Autoradiogram showing the basal, packaging-stimulated, and gp16-stimulated ATPase activities of wild-type K577, N360, and C360 domains. Concentrations of gp17, N360 and C360 domains used were 0.5  $\mu\text{M}$ . (b) Packaging-stimulated ATPase activity of each construct at varying ATP concentration. (c) Inhibition of gp17-K577 packaging by N360 and C360 domains. The gp17-K577 concentration was kept at 1.5  $\mu\text{M}$  and the concentration of the domains was varied (0.5–6  $\mu\text{M}$ ). Other experimental conditions were the same as described in the legend to Figure 6.

gp17 does appear to interact with the portal although the interacting aa must reside more internal in the C-domain polypeptide chain (see below).

Up to about 30% of the proheads could be packaged in the defined system as opposed to 0.01–1% in the crude *in vitro* systems described earlier.<sup>21</sup> Thus it appears that the defined system isolates the relatively efficient DNA packaging step from the inefficient post-packaging assembly steps. The packaging efficiency was calculated using the assumption that each prohead is filled with one DNA molecule (see footnote†). However, as observed earlier,<sup>29</sup> it is likely that at least some of the proheads are filled with more than one plasmid DNA molecule. Since the size of pAD10 plasmid is 29 kb, after packaging one molecule, the prohead could continue to package up to five or six additional pAD10 molecules to fill the capsid container. Therefore, at the other extreme, if each prohead is filled to completion, the packaging efficiency would be 5–6%, not 30%. This point and the mechanism of discontinuous packaging, a very interesting phenomenon that will have implications to the evolution of viral packaging systems, require further investigation.

All icosahedral dsDNA bacteriophages undergo prohead expansion, a striking morphogenetic event that leads to significant rearrangement of the major capsid subunit interactions.<sup>35,36</sup> A greatly stabilized T4 capsid with ~50% increased inner volume results following expansion. Confirming our previous data,<sup>21</sup> the expanded ELPs are the most active

species for DNA packaging in the defined system. Although unexpanded ESPs could be isolated as a mixture of ESPs and ELPs, these proheads were less active and the yields were variable. The fact that pure ELPs, including the 12 year old stored ELPs, efficiently packaged in the defined system reaffirms the hypothesis that prohead expansion as such is not mechanistically (or energetically) coupled to DNA packaging. While prohead expansion and packaging go hand in hand *in vivo*, and in fact expansion apparently occurs after 8–25% of DNA is packaged,<sup>37,38</sup> the biological role of expansion must be reconciled with a function other than the DNA packaging mechanism.

Packaging in the defined system is preferentially, and non-specifically, initiated at the ends of the linear dsDNA. This was commonly observed in other phage defined systems, for example SPP1.<sup>25</sup> No discrimination was evident based on the DNA sequence or the type of end used. The fact that the length of the packaged DNA corresponded to the length of linear DNA substrate used suggests that cutting and initiation at an internal site was not highly significant; if so, a substantial smear of DNA would have been evident in addition to the linear form. However, cutting very near (a few base-pairs) to the end cannot be ruled out, since the agarose gel would not have resolved cleaved fragments having small differences in molecular size.

Packaging of circular DNA molecules suggests that gp17, in the absence of an end, can randomly cut the DNA and initiate packaging at the newly generated end. This resulted in, as evident from

restriction digestion analysis of the packaged DNA, circularly permuted ends, which is consistent with the strictly headful packaging by phage T4. While a non-specific endonuclease contaminant cannot be ruled out, the evidence suggests that the ends are likely generated by gp17: (i) gp17 is well documented to possess a non-specific endonuclease activity, which cleaves circular plasmid DNAs *in vivo*;<sup>39–41</sup> (ii) a variety of circular plasmid DNAs, pAD10 (29 kb), pET28b (5.4 kb), pUC19-GFP (3.3 kb), and pUC19 (2.7 kb) were packaged; (iii) gp17 purified through a DNA-cellulose column, which should have removed any contaminating endonuclease (gp17 does not bind to DNA-cellulose), was as active for packaging circular DNA (data not shown); (iv) a defined *in vitro* DNA cleavage assay was recently developed using gp17, which showed similar cleavage pattern as the *in vivo* gp17-nuclease; in this assay, the nuclease was specifically inhibited by gp16, which would not be the case if it were a contaminating nuclease (T. I. Alam and V. B. R., unpublished data). However, the nuclease issue requires further investigation, which is currently underway.

The small terminase was not only unnecessary for defined *in vitro* DNA packaging but also strongly inhibitory. The dispensability of gp16 *in vitro* was observed before<sup>15,42</sup> and is not surprising because gp17 as such seems to efficiently attach to the ends of the linear DNA and initiate packaging. Therefore, while gp16's role to recognize packaging initiation site on viral concatemeric DNA is indispensable *in vivo*, it is not so for *in vitro* packaging of already cut linear molecules.

The inhibitory nature of gp16 is intriguing at first glance, since gp16 is known to enhance the packaging of T4 DNA by about 100-fold in the extract-based *in vitro* packaging system.<sup>15,28</sup> However analysis of these two systems points to insights on the mechanism of headful packaging initiation. In the extract-based system, the externally added T4 DNA is recombined with the endogenous concatemeric DNA by the highly proficient T4 recombination system. Packaging occurs not from the ends of the linear T4 DNA but largely from the ends generated by cutting of the recombined concatemeric DNA. In fact, using genetic markers, it was shown that >90% of the *in vitro* packaged DNA was through recombination/cutting mechanism.<sup>15</sup> Black and co-workers reported that interaction of gp17 with the late transcription Sigma factor, gp55, switches DNA metabolism from late transcription to DNA packaging.<sup>43</sup> Gp16 enhancement of this mode of packaging is consistent with its proposed role in recognition of a *pac* site,<sup>42</sup> interaction with gp17 to form holoterminase,<sup>19,20</sup> and assembly of a macromolecular packaging complex.<sup>6</sup> However, in the defined system, in the absence of partners of late transcription machinery, interaction of gp16 with the dsDNA, DNA ends, and/or gp17 leads to the formation of aberrant non-productive complexes that are unable to efficiently link the DNA to the prohead portal and initiate packaging.

Although it is widely believed that stimulation of translocating ATPase following the assembly of a functional packaging motor is central to the packaging process, there has been no direct evidence in any phage system that links DNA translocation to a specific ATPase site. Packaging-stimulated ATPase was observed in phages  $\lambda$  and Phi-29 defined systems; however the background non-packaging ATPase activity was quite high in the  $\lambda$  system<sup>18,32</sup> and its linkage to DNA translocation has not been specifically addressed in the Phi-29 system.<sup>44</sup> Moreover, in the case of  $\lambda$  terminase, definitive evidence was lacking as to which of the three ATPase sites (two in gpA and one in gpNu1) powers translocation. In the defined T4 system, neither the proheads nor gp17 exhibited non-packaging basal ATPase activity. The small terminase, which would have greatly contributed to ATPase stimulation, is completely dispensable in the defined system, making it an ideal set-up to analyze the translocating ATPase. Our data clearly showed that robust ATPase stimulation occurred only when all the motor components, proheads, gp17, and DNA, are engaged in an active packaging mode. Either proheads or DNA as such showed mild stimulation over the basal gp17-ATPase level. Mutants in the N-terminal gp17-ATPase could neither stimulate ATPase nor package DNA. In particular, the E256Q (catalytic carboxylate) and D255E-E256D (Walker B and catalytic carboxylate) mutants, which bind to ATP with equal or greater affinity than the wild-type<sup>16,17</sup> (A. R. Al-Zahrani and V. B. R., unpublished data), showed no packaging. The fact that these mutants, being trapped in an ATP-bound conformation, neither exhibited packaging ATPase stimulation nor encapsidated DNA, points to an energetic connection between the N-terminal ATPase center and DNA translocation. Not surprisingly, the catalytic signatures of this ATPase, not of the additional ATPase site(s) present elsewhere in the terminase genes, are highly conserved among >200 large terminase sequences analyzed thus far.<sup>14</sup>

Neither the individual ATPase or nuclease domains nor a mixture of both the domains exhibited stimulated ATPase or packaged DNA. An important observation is that the N-360 ATPase domain, which showed even greater gp16-mediated ATPase stimulation than the full-length protein, did not show any packaging-mediated ATPase stimulation (i.e. in the presence of proheads and DNA). On the other hand, both the domains, in particular the C-domain strongly inhibited gp17-K577-dependent DNA packaging. These data suggest that interaction of the C-domain with the prohead portal, and communication between the C and N-domains are essential in order to couple DNA translocation and ATP hydrolysis. It is interesting that, although both gp16 and DNA translocation stimulate the same N-terminal ATPase, stimulation is signaled *via* different pathways, gp16 stimulation through interaction with the N-domain, and packaging stimulation through the C-domain-portal interaction.

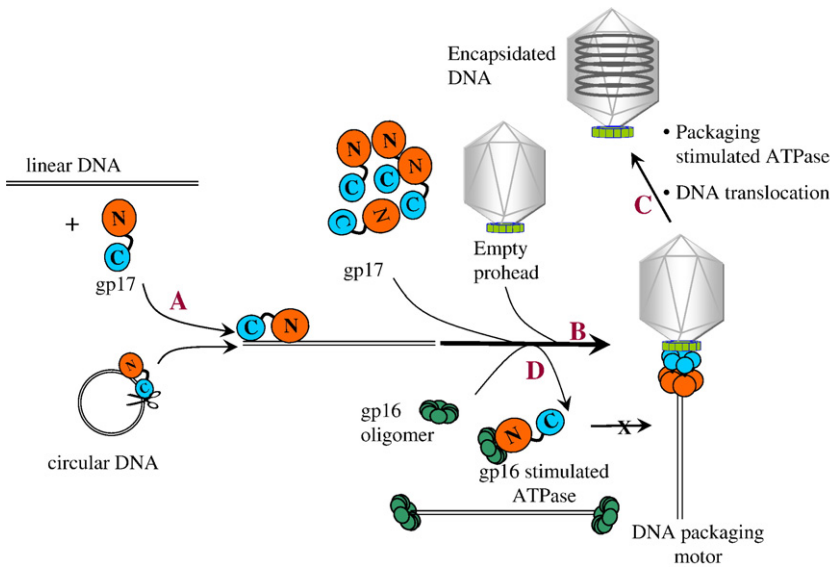


**Figure 8.** The core pathway for assembly of phage T4 DNA packaging motor. The gp17 N and C-domains are shown in red and cyan, respectively. The gp16 is shown in green as an octamer. The green collar at the unique vertex of prohead represents the dodecameric gp20 portal. The nucleic acid cutting of circular DNA is shown by using scissors symbol. Partially packaged DNA is represented as a barrel inside the prohead. The depicted stoichiometry of p16 oligomer as an octamer and gp17 as a pentamer are speculative. See Discussion for details.

A core DNA packaging model, which is consistent with the experimental data, but necessarily speculative in certain aspects, is shown in Figure 8. The large terminase attaches to the ends of the linear dsDNA through the DNA cutting C-domain (A). This is likely supported by additional interactions between the N-domain and the adjacent dsDNA (recent evidence suggests that the N-domain binds to DNA; T. I. Alam and V. B. R., unpublished data). If the substrate is a circular plasmid, the C-domain non-specifically cuts the DNA at a random site and attaches itself to the newly generated end. The gp17–DNA complex then interacts with the portal through the C-domain and assembles into an oligomeric complex (B, there is genetic and biochemical evidence for gp17–portal interaction<sup>45</sup>). As was observed, a threshold concentration of gp17 is necessary in order to assemble the macromolecular packaging motor. *In vivo* however, these steps are regulated through interaction of gp17 with gp16 as well as the T4 late transcription/recombination proteins,<sup>19,43</sup> which imparts specificity and efficiency to packaging initiation on the concatemeric viral genome. If as in the defined packaging system only gp16 but not the late transcription/recombination partners is present, gp16 interaction with DNA and/or gp17 leads to non-productive complexes resulting in greatly diminished packaging initiation (D). The assembly of packaging motor, resulting in the integration of prohead portal, DNA and terminase functionalities, triggers stimulation of N-domain ATPase and the coupled DNA translocation (C). If only the N-domain ATPase is present, or if the domains are split, although the ATPase is stimutable (by gp16), the packaging-specific signaling through C-domain–portal interaction would be missing or interrupted. Then the motor can neither prime ATPase stimulation nor sponsor DNA translocation. Thus, cross-communication among the components of the packaging machinery, initially between gp16, gp17, and late transcription/recombination partners,<sup>15,19,43</sup> and later between portal,

gp17 C-domain, and N-domain, is crucial to orchestrate the complex process of DNA packaging initiation and translocation. Clearly, the defined system bypassed the requirement for the former interactions, allowing more direct analysis of DNA translocation.

Recent structural modeling data showed that all well-characterized large terminases analyzed (e.g.  $\lambda$  gpA, Phi-29 gp16, HSV UL15, T3 gp19; B. Draper and V. B. R., unpublished data) consist of the classic parallel  $\beta$ -strand core Rec-A ATPase fold, which orients Walker A, Walker B and other catalytic residues into the ATP binding pocket. This model closely fits with the solved ATPase domain structures of SF1 and SF2 helicases.<sup>46</sup> Combined with the biochemical evidence presented here, the energetic linkage between this common ATPase center and DNA translocation is compelling and definitive. With the establishment of the simplified two-component packaging system, the intermediates of DNA translocation as well as the biophysical features of the T4 packaging motor are now amenable to structural and single molecule investigations, which should delineate the dynamic mechanisms of ATP energy transduction in viral DNA translocation.

## Materials and Methods

### Bacteria, phage, and DNAs

*Escherichia coli* P301 (*sup*<sup>-</sup>) strain was used for preparation of phage T4 proheads. *E. coli* BL21 (DE3) pLysS was used to over-express all gp17 constructs.<sup>47</sup> The *17Q425am-18amE18.rIIdel* was constructed by standard phage crosses.<sup>21</sup> Construction of T4 gp17 clones in pET vectors was described earlier.<sup>13–17</sup> Construction of the 29 kb P1-pBR hybrid vector, pAD10, was described earlier.<sup>26</sup> The pAD10 and pET28b DNA were linearized by digestion with BamHI, which cuts at a unique site in the plasmid. The linear DNA was concentrated by ammonium acetate-isopropanol precipitation and dissolved in sterile water. Phage T4 DNA was prepared by standard phenol-chloroform extraction procedure. Phage  $\lambda$  DNA was purchased

from Fermentas. Non-hydrolyzable analogs of ATP; ATP- $\gamma$ -S, AMP-PNP and AMP-CP were purchased from Sigma.

### Purification of proheads

Phage T4 produces a mixture of ELPs and ESPs upon infection with the packaging defective mutant, *17am18amrII*. Infection at 37 °C yields largely ELPs, whereas at 25 °C largely ESPs are produced.<sup>21</sup> Since our previous data demonstrated that ELPs, but not ESPs, are more active for *in vitro* DNA packaging, the cultures were grown at 37 °C in order to enrich for ELPs. *E. coli* P301 grown at 37 °C on 50:50 LB:M9A medium (150 ml) was infected with *17am18amrII* at a multiplicity of 2.5 and super-infected at the same multiplicity 7 min later. The culture was grown for about 45 min at 37 °C and harvested by centrifugation at 7000 rpm for 12 min. The pellet was resuspended in 5 ml of buffer-I (50 mM Tris-HCl (pH 7.4), 5 mM MgCl<sub>2</sub>, 3 mM  $\beta$ -mercaptoethanol) plus 10  $\mu$ g/ml DNase containing 20 drops of chloroform and incubated at 37 °C for 30 min. To this, 20 ml of buffer-II (the same as above plus 50 mM NaCl) was added and the sample was centrifuged at 7000 rpm for 12 min. The supernatant containing proheads was centrifuged at 18,000 rpm for 45 min. The pellet was resuspended in buffer-II, and the low and high speed centrifugations were repeated. The sample was then resuspended in 400–600  $\mu$ l of buffer-II and purified by high pressure Mono-Q column chromatography (Mono Q 5/50 GL, GE Healthcare) using a 0–400 mM linear NaCl gradient on an AKTA-FPLC chromatography system (GE Healthcare). The proheads eluted as two major peaks; a sharp peak (Peak-I) consisting of pure ELPs and a broad peak (Peak-II) consisting of mostly ELPs and a small fraction of ESPs. It is likely that this fraction originally consisted of more ESPs, which were expanded during and after purification. The proheads were concentrated by centrifugation at 18,000 rpm for 1 h and resuspended in buffer-I and stored at –70 °C.

### Expanded status of proheads

The main differences between ELPs and ESPs are: (i) ELPs are stable to SDS treatment at room temperature whereas ESPs are completely dissociated; and (ii) ELPs have the outer capsid proteins, Hoc and Soc, whereas ESPs do not. The former property was used to distinguish the concentration of ELPs *versus* ESPs in a given sample.<sup>21</sup> The samples were treated with SDS-sample buffer both at room temperature and at boiling temperature followed by electrophoresis on a SDS-PAGE. The amount of major capsid protein (gp23\*; 49 kDa) in the room-temperature (unboiled) lane gave the fraction of ESPs, whereas the same in the boiled lane gave the total number of proheads. ELPs and ESPs were quantified by determining the intensity of gp23\* in the boiled and unboiled lanes and comparing with that from a known number of phage particles (see below).

### Purification of terminase proteins

Wild-type gp17 (K577: aa 1–577), ATPase domain (N360: aa 1–360), nuclease domain (C360: aa 360–577), Walker-A mutant (K1266G), Walker-B mutant (D255E), catalytic carboxylate mutant (E256Q), and double mutants (D255E-E256D, D255E-E256Q), and gp16 were purified by a combination of Ni-agarose, ion-exchange, and size-exclusion chromatographies as described.<sup>15–17,20</sup>

Wild-type gp17 and E255D-E256Q mutant were truncated at K577, whereas K166G, D255E, E256Q, and D255E-E256D mutants were purified as full-length (1–610 aa) proteins. The full-length protein was cleaved by non-specific proteolysis during purification. Therefore, two–three bands (the full-length protein and one or two shorter forms) were seen by SDS-PAGE (Figure 1(a)). The K577 on the other hand showed a single sharp band.

### Quantification of packaging components

Purified proteins and proheads were electrophoresed on a 12% (w/v) SDS-PAGE and the gels were stained with Coomassie blue, scanned with laser densitometer (PDSI scanner; GE Healthcare) and quantified using Imagequant 5.2 software.<sup>48</sup> A known amount of *hoc*<sup>–</sup>*soc*<sup>–</sup> phage was used in each experiment and the number of prohead particles in a given sample was quantified by computing the intensity of the gp23\* bands. Packaged DNAs were resolved on 0.8% (w/v) agarose gels, visualized with ethidium bromide and the amount of DNA was quantified using Eagle Eye II imaging system (Stratagene).

### Defined *in vitro* DNA packaging assays

In a typical assay, the purified terminase protein (1.5  $\mu$ M) and proheads ( $2 \times 10^9$  prohead particles) were incubated in a reaction mixture (20  $\mu$ l) containing 50 mM Tris-HCl (pH 7.5), 5 mM MgCl<sub>2</sub>, 1 mM spermidine, 1 mM putrescine, 5% (w/v) polyethylene glycol (Fluka), 1 mM ATP, 100 mM NaCl and 300–600 ng of linear pAD10 DNA (29 kb;  $1 \times 10^{10}$ – $2 \times 10^{10}$  DNA molecules) for 45 min at room temperature (~28 °C). DNase I (Sigma) was added to a final concentration of 0.5  $\mu$ g/ $\mu$ l and incubated for 30 min at 37 °C. Proteinase K (Fermentas) was added to a final concentration of 0.5  $\mu$ g/ $\mu$ l in 50 mM EDTA (pH 8.0), 0.2% SDS and incubated for 30 min at 65 °C. Gel loading buffer was added and the samples were electrophoresed on a 0.8% agarose gel for 2–3 h at 100 V.

### Packaging-ATPase assays

The purified terminase proteins (0.5  $\mu$ M), either alone or with DNA (300 ng), prohead ( $2 \times 10^9$  particles) and/or gp16 (4  $\mu$ M) were incubated in the above-mentioned *in vitro* packaging reaction mixture (20  $\mu$ l) containing 0.125–2 mM unlabelled ATP and 75 nM of [ $\gamma$ -<sup>32</sup>P]ATP (spec. act. 3000 Ci/mmol; GE Healthcare) at 37 °C for 30 min. After incubation, 0.6  $\mu$ l samples were resolved by TLC and autoradiography was performed. Quantification of ATP hydrolysis was performed by phosphorimaging (Storm 820, Molecular Dynamics).<sup>6,20</sup> To obtain substrate saturation curves, the concentration of unlabelled ATP was varied (0.125–2 mM), and the concentration of [ $\gamma$ -<sup>32</sup>P]ATP was fixed at 75 nM. From the <sup>32</sup>P<sub>i</sub> value, total [P<sub>i</sub>] produced was determined and substrate saturation curves were plotted using Sigma-Plot 8.0 software.

### Acknowledgements

We thank Dr Lindsay Black from the University of Maryland Medical School for communicating results prior to publication and critical review of

the manuscript. We gratefully acknowledge the grant support (MCB-423528) to V.B.R.'s laboratory by the National Science Foundation.

## References

- Black, L. W. (1988). DNA packaging in dsDNA bacteriophage. In *The Bacteriophages* (Calendar, R., ed), pp. 321–363, Plenum Press, NY.
- Rao, V. B. & Black, L. W. (2005). DNA packaging in bacteriophage T4. In *Viral Genome Packaging Machines: Genetics, Structure, and Mechanism* (Catalano, C. E., ed), pp. 40–58, Landes Bioscience, Georgetown, TX.
- Feiss, M. & Catalano, C. E. (2005). Bacteriophage lambda terminase and the mechanisms of viral DNA packaging. In *Viral Genome Packaging Machines: Genetics, Structure, and Mechanism* (Catalano, C. E., ed), pp. 5–39, Landes Bioscience, Georgetown, TX.
- Jardine, P. J. & Anderson, D. L. (2006). DNA packaging in double-stranded DNA phages. In *The Bacteriophages* (Calendar, R., ed), pp. 49–65, Oxford University Press, Oxford, UK.
- Lander, G. C., Tang, L., Casjens, S. R., Gilcrease, E. B., Prevelige, P., Poliakov, A. *et al.* (2006). The structure of an infections P22 Virion shows the signal for heedful DNA packaging. *Science*, **312**, 1791–1795.
- Kondabagil, K. R. & Rao, V. B. (2006). A critical coiled coil motif in the small terminase, gp16, from bacteriophage T4: insights into DNA packaging initiation and assembly of packaging motor. *J. Mol. Biol.* **358**, 67–82.
- Hendrix, R. W. (1978). Symmetry mismatch and DNA packaging in large bacteriophages. *Proc. Natl Acad. Sci. USA*, **75**, 4779–47783.
- Simpson, A. A., Tao, Y., Leiman, P. G., Badasso, M. O., He, Y., Jardine, P. J. *et al.* (2000). Structure of the bacteriophage phi29 DNA packaging motor. *Nature*, **408**, 745–750.
- Smith, D. E., Tans, S. J., Smith, S. B., Grimes, S., Anderson, D. L. & Bustamante, C. (2001). The bacteriophage straight phi29 portal motor can package DNA against a large internal force. *Nature*, **413**, 748–752.
- Chemia, Y. R., Aathavan, K., Michaelis, J., Grimes, S., Jardine, P. J., Anderson, D. L. & Bustamante, C. (2006). Mechanism of force generation of viral DNA packaging motor. *Cell*, **122**, 683–692.
- Guo, P., Peterson, P. J. & Anderson, D. (1987). Prohead and DNA-gp3-dependent ATPase activity of the DNA packaging protein gp16 of bacteriophage phi 29. *J. Mol. Biol.* **197**, 229–236.
- Morita, M., Tasaka, M. & Fujisawa, H. (1994). Analysis of functional domains of the packaging proteins of bacteriophage T3 by site-directed mutagenesis. *J. Mol. Biol.* **235**, 248–259.
- Rao, V. B. & Mitchell, M. S. (2001). The N-terminal ATPase site in the large terminase protein gp17 is critically required for DNA packaging in bacteriophage T4. *J. Mol. Biol.* **314**, 401–411.
- Mitchell, M. S., Matsuzaki, S., Imai, S. & Rao, V. B. (2002). Sequence analysis of bacteriophage T4 DNA packaging/terminase genes 16 and 17 reveals a common ATPase center in the large subunit of viral terminases. *Nucl. Acids Res.* **30**, 4009–4021.
- Leffers, G. & Rao, V. B. (2000). Biochemical characterization of an ATPase activity associated with the large packaging subunit gp17 from bacteriophage T4. *J. Biol. Chem.* **275**, 37127–37136.
- Mitchell, M. S. & Rao, V. B. (2006). Functional analysis of the bacteriophage T4 DNA packaging ATPase motor. *J. Biol. Chem.* **281**, 518–527.
- Goetzinger, K. R. & Rao, V. B. (2003). Defining the ATPase center of bacteriophage T4 DNA packaging machine: requirement for a catalytic glutamate residue in the large terminase protein gp17. *J. Mol. Biol.* **331**, 139–154.
- Dhar, A. & Feiss, M. (2005). Bacteriophage lambda terminase: alterations of the high affinity ATPase affect viral DNA packaging. *J. Mol. Biol.* **347**, 71–80.
- Baumann, R. G. & Black, L. W. (2003). Isolation and characterization of T4 bacteriophage gp17 terminase, a large subunit multimer with enhanced ATPase activity. *J. Biol. Chem.* **278**, 4618–4627.
- Kanamaru, S., Kondabagil, K., Rossmann, M. G. & Rao, V. B. (2004). The functional domains of bacteriophage t4 terminase. *J. Biol. Chem.* **279**, 40795–40801.
- Rao, V. B. & Black, L. W. (1985). DNA packaging of bacteriophage T4 proheads *in vitro*. Evidence that prohead expansion is not coupled to DNA packaging. *J. Mol. Biol.* **185**, 565–578.
- Carrascosa, J. L. & Kellenberger, E. (1978). Head maturation pathway of bacteriophage T4 and T2. III. Isolation and characterization of particles produced by mutants in gene 17. *J. Virol.* **25**, 831–844.
- Hwang, Y. & Feiss, M. (1995). A ded system for *in vitro* lambda DNA packaging. *Virology*, **211**, 367–376.
- Gaussier, H., Yang, Q. & Catalano, C. E. (2006). Building a virus from scratch: assembly of an infectious virus using purified components in a rigorously defined biochemical system. *J. Mol. Biol.* **353**, 529–539.
- Oliveira, L., Alonso, J. C. & Tavares, P. (2005). A defined *in vitro* system for DNA packaging by the bacteriophage SPP1: insights into the headful packaging mechanism. *J. Mol. Biol.* **353**, 529–539.
- Pierce, J. C. & Sternberg, N. (1992). Using bacteriophage P1 system to clone high molecular weight genomic DNA. *Methods Enzymol.* **216**, 549–574.
- Rao, V. B. & Black, L. W. (1988). Cloning, overexpression and purification of the terminase proteins gp16 and gp17 of bacteriophage T4. Construction of a defined *in vitro* DNA packaging system using purified terminase proteins. *J. Mol. Biol.* **200**, 475–488.
- Black, L. W. (1981). *In vitro* packaging of bacteriophage T4 DNA. *Virology*, **113**, 336–344.
- Leffers, G. & Rao, V. B. (1996). A discontinuous headful packaging model for packaging less than headful length DNA molecules by bacteriophage T4. *J. Mol. Biol.* **258**, 839–850.
- Ishii, T. & Yanagida, M. (1977). The two dispensable structural proteins (soc and hoc) of the T4 phage capsid: their purification and properties, isolation and characterization of the defective mutants, and their binding with the defective heads *in vitro*. *J. Mol. Biol.* **109**, 487–514.
- Camacho, A. G., Gual, A., Lurz, R., Tavares, P. & Alonso, J. C. (2003). *Bacillus subtilis* bacteriophage SPP1 DNA packaging motor requires terminase and portal proteins. *J. Biol. Chem.* **278**, 23251–23259.
- Yang, Q. & Catalano, C. E. (2003). Biochemical characterization of bacteriophage lambda genome packaging *in vitro*. *Virology*, **305**, 276–287.
- Morita, M., Tasaka, M. & Fujisawa, H. (1995). Structural and functional domains of the large subunit of the bacteriophage T3 DNA packaging enzyme: importance of the C-terminal region in prohead binding. *J. Mol. Biol.* **245**, 635–644.
- Yeo, A. & Feiss, M. (1995). Specific interaction of

- terminase, the DNA packaging enzyme of bacteriophage lambda, with the portal protein of the prohead. *J. Mol. Biol.* **245**, 141–150.
35. Jardine, P. J., McCormick, M. C., Wallace, C. L. & Coombs, D. H. (1998). The bacteriophage T4 DNA packaging apparatus targets the unexpanded prohead. *J. Mol. Biol.* **284**, 647–659.
  36. Black, L. W., Showe, M. K. & Steven, A. C. (1994). Morphogenesis of the T4 head. In *Molecular Biology of Bacteriophage T4* (Karam, J. D., ed), pp. 218–258, ASM Press, Washington, DC.
  37. Shibata, H., Fujisawa, H. & Minagawa, T. (1987). Characterization of the bacteriophage T3 DNA packaging reaction *in vitro* in a defined system. *J. Mol. Biol.* **196**, 845–851.
  38. Hohn, B. & Hohn, T. (1974). Activity of empty, headlike particles for packaging of DNA of bacteriophage lambda *in vitro*. *Proc. Natl Acad. Sci. USA*, **71**, 2372–2376.
  39. Rentas, F. J. & Rao, V. B. (2003). Defining the bacteriophage T4 DNA packaging machine: evidence for a C-terminal DNA cleavage domain in the large terminase/packaging protein gp17. *J. Mol. Biol.* **334**, 37–52.
  40. Bhattacharyya, S. P. & Rao, V. B. (1993). A novel terminase activity associated with the DNA packaging proteins gp17 of bacteriophage T4. *Virology*, **196**, 34–44.
  41. Kuebler, D. & Rao, V. (1998). Functional analysis of the DNA packaging /terminase protein gp17 from bacteriophage T4. *J. Mol. Biol.* **281**, 803–814.
  42. Lin, H., Simon, M. N. & Black, L. W. (1997). Purification and characterization of the small subunit of phage T4 terminase, gp16, required for DNA packaging. *J. Biol. Chem.* **272**, 3495–3501.
  43. Malys, N., Chang, D. Y., Baumann, R. G., Xie, D. M. & Black, L. W. (2002). A bipartite bacteriophage T4 soc and hoc randomized peptide display library: detection and analysis of phage T4 terminase (gp17) and late o factor (gp55) interaction. *J. Mol. Biol.* **319**, 289–304.
  44. Huang, L. P. & Guo, P. (2003). Use of acetone to attain highly active and soluble DNA packaging protein Gp16 of Phi29 for ATPase assay. *Virology*, **312**, 449–457.
  45. Lin, H., Rao, V. B. & Black, L. W. (1999). Analysis of capsid portal protein and terminase functional domains: interaction sites required for DNA packaging in bacteriophage T4. *J. Mol. Biol.* **334**, 37–52.
  46. Delagoutte, E. & von Hippel, P. H. (2002). Helicase mechanisms and the coupling of helicases within macromolecular machines. Part I: structures and properties of isolated helicases. *Quart. Rev. Biophys.* **35**, 431–478.
  47. Studier, F. W., Rosenberg, A. H., Dunn, J. J. & Dubendorff, J. W. (1990). Use of T7 RNA polymerase to direct expression of cloned genes. *Methods Enzymol.* **185**, 60–89.
  48. Shivachandra, S. B., Rao, M., Janosi, L., Sathaliyawa, T., Matyas, G. R., Alving, C. R., Leppla, S. H. & Rao, V. B. (2006). *In vitro* binding of anthrax protective antigen on bacteriophage T4 capsid surface through hoc-capsid interactions: a strategy for efficient display of large full-length proteins. *Virology*, **345**, 190–198.

*Edited by M. Gottesman*

(Received 15 June 2006; received in revised form 20 August 2006; accepted 21 August 2006)  
Available online 25 August 2006